A Polytopal Element Framework for Improved Solution Accuracy and Robustness

By

Brian Doran Giffin
B.S. (University of California, Davis) 2013
M.S. (University of California, Davis) 2014

Dissertation

Submitted in partial satisfaction of the requirements for the degree of

Doctor of Philosophy

in

Civil and Environmental Engineering

in the

Office of Graduate Studies

of the

University of California

Davis

Approved:

Mark M. Rashid, Chair

N. Sukumar

Boris Jeremić

Committee in Charge

2017

To Lyle . . .

for teaching me how to think deeply, to analyze new information objectively, and to appreciate the complexity and nuanced beauty in all things.

And to Nancy . . .

for inspiring me to explore my creativity, for giving me canvases to paint on, and the confidence to paint, without fear of failure.

Contents

List of Figures

List of Tables

Abstract

A Polytopal Element Framework for
Improved Solution Accuracy and Robustness

A high-level discussion of the fundamental problems accompanying finite element discretizations in the form of locking, addressing the scope of the work under consideration.

Acknowledgments

Many thanks to the following: Professor Amit Kanvinde who inspired much of my initial motivation for applying to graduate school; Professor N. Sukumar for exposing me to the realm of computational solid mechanics; Dr. Joseph Bishop at Sandia for being involved in my early (and continuing) development in the field of solid mechanics; Professor Mark Rashid who turned my spark of interest in the subject into a roaring fire of passion; Dr. Steven Wopschall and Mr. Omar Hafez for being my mentoring older brothers throughout my journey in graduate school; Mr. Subhajit Banerjee and Mr. Eric Chin whose fruitful discussions assisted greatly in developing a personal sense of calm and confidence prior to my qualifying examination; Professor Yannis Dafalias, Professor John Bolander, and Professor Elbridge Puckett, whose enthusiasm as lecturers and courtesy as QE examiners were indespensible; Dr. Joseph Jung, Dr. Kendall Pearson, Dr. Nathan Crane, Mr. Mark Merewether, Dr. Michael Tupek, and the whole of the Sierra Solid Mechanics Team at Sandia who introduced me to the fascinations of code development; Ms. Carly Arthur, Mr. Sam Mish, and Ms. Aimée Sylvia whose conversations as fellow class-mates and advisees were incredibly helpful and insightful; and foremost to Ms. Maha Kenawy, who has served as my primary role-model and source of inspiration for completing this thesis – I love you.

Chapter 1

Introduction

For decades, finite element methods have been the foremost tool for engineers and physicists to model the deformation of solid bodies. Numerous extensions of the method have been developed in an effort to model more complex physical processes, including nonlinear kinematic and material behavior.

Despite these advances, traditional finite element methods have been plagued by recurrent issues of numerical accuracy pertaining to locking and poor mesh quality. Various strategies have been proposed to overcome some of these issues, though few have been able to address the underlying problem of element distorsion sensitivity.

This thesis presents a polytopal element framework to address the aforementioned issues. The use of arbitrary polygonal and polyhedral shapes in place of the standard element shapes used in FEM seeks to address the issue of distorsion sensitivity directly, obviating issues of meshing and mesh quality, while maintaining many of the desirable features of the FEM.

1.1 Historical Development

According to [14], finite element methods originated in the 1950s to address challenges related to the engineering design of aircraft. More rigorous mathematical justifications of the method were developed later on, and its usage permeated to other fields of study (namely, in structural engineering applications). Following the advent of isoparametric element formulations, displacement-based finite element methods gained widespread

popularity, though most early applications considered only linear kinematic and material behavior. Subsequently, advanced solution methodologies were developed to accomodate various sources of nonlinearity, including finite deformations, nonlinear constitutive behavior, and contact.

Over half a century after its initial development, the finite element method is still widely used, and recognized as the industry standard method for modeling complicated structural systems. It's reigning popularity can be attributed to several desirable features of the method:

1.) The compact support property of the isoparametric basis functions helps to facilitate more efficient solution methodologies.

2.) The kronecker delta property and precise description of mesh boundaries allow for a relatively straightforward application of boundary conditions and contact constraints.

3.) Numerical quadrature on element domains derived from product Gauss rules balances accuracy, efficiency, and stability, which also accomodates nonlinear kinematic and material behavior.

However, despite these advantageous characteristics, finite element methods have suffered from two major (related) issues:

1.) Standard element formulations are prone to the effects of numerical locking phenomena, which can significantly degrade the accuracy of the method. These issues are more prevalent for low-order elements, and especially so for linear triangles and tetrahedra. Moreover, very thin or distorted elements tend to exhibit more severe pathologies.

2.) The process of meshing complex geometries is encumbered by the aforementioned concerns over locking, to the extent that it becomes difficult – if not impossible to produce quality discretizations using automated tools which do not require extensive human intervention.

Despite recent efforts to pursue automated quad-dominant [32] and hex-dominant [18] meshing algorithms which seek to optimize certain mesh quality metrics, the inherrent problem of element distorsion sensitivity still remains. Consequently, substantial efforts have been made to address the locking problem through a variety of different approaches, to be discussed in the following section.

1.1.1 Locking in Finite Elements

Locking, as a general phenomenon presented in [3], is characterized by a loss of solution accuracy and/or convergence for certain choices of material or discretization parameters. In mathematical terms, an approximation method is deemed *robust* if the accuracy of its numerical solution converges uniformly under mesh refinement for all values of a given problem parameter. Conversely, a method is said to exhibit *locking* if the accuracy of the solution degenerates as the chosen problem parameter approaches some limiting value.

One of the most commonly discussed and addressed forms of locking in computational solid mechanics is the issue of *volumetric locking*, wherein displacement-based element formulations suffer from a marked loss of accuracy when used to model the deformation of nearly incompressible materials. For a linear elastic material model, the parameter dependency in question relates to the Poisson's ratio of the material. Other forms of locking which are sensitive to geometric/discretization parameters include: *shear locking*, which is linked to the aspect ratio of continuum elements used to model thin geometries; *membrane locking*, which occurs in curved shell elements (see [47]); and *trapezoidal locking*, which occurs in distorted four-node quadrilateral elements (see [24]).

Early efforts to address issues pertaining to locking sought to develop more robust discretizations in the form of higher-order elements. In [2] and [40], Babuška and Suri justified the ability of high-order elements to overcome the effects of volumetric locking. Moreover, the improved convergence behavior of these elements made them an attractive option for seeking efficiency gains. Nonetheless, higher-order elements were generally seen as too complex in comparison with standard low-order elements for commercial applications. Additionally, high-order elements encounter issues when applied to explicit dynamics problems due to the relative difficulty of constructing a lumped mass matrix.

Moreover, the accuracy and convergence rate of high-order elements is degraded if the elements posess curved edges, as demonstrated in [21].

As an alternative to the standard displacement-based element formulations, some researchers have argued for the use of so-called mixed finite element methods, which provide a separate interpolation of the displacement, strain, and stress fields utilizing a 3-field Hu-Washizu variational principle in the specification of the weak form. While these methods are generally seen as robust in the face of locking (as noted in [3] and [2]), they are nonetheless subject to potential issues of stability, i.e. the Babuška-Brezzi, or inf-sup conditions (refer to [1], [5].) Mixed methods are also not as easily generalized to handle arbitrary constitutive relationships in comparison with standard FEM discretizations.

In an effort to retain some of the beneficial characteristics of mixed finite element methods, mixed assumed strain methods (alternately the method of incompatible modes) were formalized for geometrically linear problems in [36], and extended to nonlinear problems in [34] and [35]. Such methods derive from the Hu-Washizu variational principle, and rely upon energy orthogonality between the enhanced strain field and the resulting stress field to eliminate the need for independently interpolating the stress field, thereby yielding a 2-field formulation. Though the method is effective in treating a variety of geometric locking phenomena, it nonetheless suffers from spurious instability problems for both linear and nonlinear problems (see [41] and [28], respectively), even if the elements satisfy the inf-sup condition.

Other attempts to adapt mixed formulations for more general use with arbitrary material models without relying upon an interpolation of the stress field resulted in selective reduced integration (SRI) and equivalent strain projection techniques, which avoided the need for the explicit interpolation of strain or stress fields. These methods were fairly successful in overcoming the issues of volumetric locking via the so-called B-bar approach for linear problems discussed in [19], and via the F-bar approach for nonlinear problems discussed in [11]. Though these methods generally perform well, their success has been limited to the problem of volumetric locking; they are less successful with regard to treating other forms of locking, and can lead to stability problems if the strain projection

spaces are not carefully chosen.

At the opposite end of the spectrum, and in recognition of the inherrent issues of stability that tend to plauge methods that rely upon reduced integration to combat locking, orthogonal hourglass control methodologies were suggested, as in [15]. These approaches considered using low-order quadrature rules to avoid common locking phenomena, combined with artificial stiffness terms to maintain stability while preserving essential convergence characteristics. While these elements tend to be highly efficient computationally (particularly for explicit dynamic analyses), the obvious disadvantage of these approaches relates to their reliance upon user-specified artificial stiffness and viscosity parameters. Appropriate selection of these parameters is not always a trivial matter, and often warrants investigation via sensitivity analyses.

Ultimately, the foregoing methodologies have had only limited success in resolving the full spectrum of locking problems, particularly with regard to geometric locking phenomena. Moreover, many of the proposed enhancements are imited to specific element formulations (typically low-order quadrilaterals or hexahedra), and are not readily generalizable to other discretizations. To a certain extent, the propensity for locking in FEM is controlled largely by the standard isoparametric elements' sensitivity to geometric distorsion. In other words, model accuracy is too often the product of the chosen discretization. For this reason, considerable efforts have been invested in recent years towards the development of alternative discretizations and numerical methods. The merits and shortcomings of these methods are discussed in the following section.

1.1.2 Alternative Numerical Methods and Discretizations

Driven by the concerns over meshing and element quality, a wide variety of alternative approximation methods have been explored in recent decades. The general consensus amongst those pursuing the development of truly "robust" numerical methods (those which perform well regardless of the specific choice of discretization) is that there is a need for abstraction away from the kinds of discretizations used to represent the approximate solution of a PDE on a given problem domain. In particular, certain forms of discretization may be convenient from a geometric perspective in the sense that they are easy to generate,

but they may not result in a suitable approximation space for the given problem at hand.

In direct response to these considerations, so-called *meshfree* methods were developed in an effort to construct approximation spaces that are defined independently of a chosen spatial discretization. Meshfree methods encompass a broad class of approximation schemes, including smoothed particle hydrodynamics (SPH), the element-free Galerkin (EFG) method, and the reproducing kernel particle method (RKPM), among others. A majority of these methods rely upon an a priori specification of a set of weighting functions used to construct an associated set of basis functions satisfying necessary reproducibility requirements. The resulting meshfree basis yields relatively smooth solutions which are less sensitive to the specific choice and distribution of weighting functions.

However, a departure from utilizing a structured partition of the domain presents a number of challenges. Specifically, meshfree methods still require the definition of a background mesh to effect numerical integration of the weak form equations, thereby invalidating claims that the method has no need of an underlying discretization. Moreover, because the basis functions tend to be non-polynomial in form (and because they are not compactly supported/overlapping on element domains), they are more challenging to accurately integrate. Chen et. al. have proposed a means of overcoming these issues in [6] though a *variationally consistent integration* scheme.

Also, because the basis functions do not in general possess the kronecker delta property, the application of boundary conditions and contact constraints becomes less straightforward. Several techniques have been proposed to handle this issue, including Lagrange multiplier methods, Nitsche's method, and mesh blending at domain boundaries.

In contrast, Discontinuous Galerkin (DG) methods have attracted the attention of researchers in the field of numerical methods development due to their represention of solution fields as piece-wise polynomials over individual elements, resulting in solution discontinuities at element boundaries. To guarantee stability, DG methods rely upon the inclusion of penalty terms which seek to minimize these discontinuities. DG methods are advantageous in that they may accomodate arbitrary element shapes, provided an appropriate numerical integration scheme can be defined over the element domain. Moreover,

DG methods exhibit desireable distorsion robustness characteristics.

However, the DG approaches have not obviated the usage of the canonical FEM and related methodologies for a number of reasons. One commonly cited reason relates to the fact that DG methods can become sensitive to the choice of penalty parameters used to weakly enforce inter-element continuity and boundary conditions; the selection of these parameters is problem dependent. Additionally, DG methods tend to suffer from poor numerical conditioning problems if the discretization does not conform with relatively stringent regularity requirements, thereby limiting the types of discretizations used with the method.

The more recent "weak Galerkin" finite element method first introduced by Wang and Ye for elliptic problems in [45], and for parabolic equations by Li and Wang in [22], pursues the discretization of a (2D) problem domain into arbitrary polygonal elements. The method considers an associated space of "weak functions" defined on the elements and their edges, such that functions defined on element domains are related to functions defined on the element's edges via a "discrete weak gradient operator." In general, the spaces of functions under consideration on the element interiors and edges are typically low-order polynomials (commonly just constants). However, there are some non-trivial choices that must be made regarding an optimal selection of these polynomial spaces for the sake of computational efficiency, which is discussed in more detail in reference [27]. Within the published literature, there appears to be little discussion regarding numerical quadrature, ostensibly because exact quadrature rules exist for simplicial geometries, which are most commonly used with the method. Additionally, the method has so-far only been applied to the solution of linear problems.

The computational accuracy of the weak Galerkin approach has been explored by Mu et. al. in [25], showing that for certain problems, the weak Galerkin method converges at rates comparable to those of the standard FEM. Lin et. al. performed a comparative study between the weak Galerkin (WG), discontinuous Galerkin (DG), and mixed finite element (MFEM) methods in [23], demonstrating some of the competitive and desirable characteristics of WG in contrast to DG or MFEMs (e.g. no need for penalty parameters,

and definiteness of the resulting linear system of equations).

Despite its generality, the method had only been extensively studied and applied to triangular or tetrahedral meshes, until Mu et. al. adapted the method for use on polytopal meshes in [26] and [27], albeit with a number of shape regularity restrictions placed on the elements. In general, the implementation of WG considers the mesh degrees of freedom as belonging to both the elements and their edges, however in [27] it is noted that the local element degrees of freedom can be expressed in terms of the bounding edge degrees of freedom to improve computational efficiency.

A modified approach for solving Poisson's equation was also proposed by Wang et. al. in [46], which sought to express functions on edges only implicitly. This modified approach, however, requires the inclusion of an additional term in the weak form which penalizes jumps in the solution value at element boundaries, similiar to a discontinuous Galerkin method. The key advantage of this approach is that it successfully reduces computational expense by eliminating the need for having degrees of freedom belonging to the edges of the mesh, albeit at the cost of introducing a dependence upon the choice of a penalty parameter.

In the wake of these investigations, it became clear that many of the desirable properties of the FEM (compact support, kronecker delta, quadrature efficiency, and inter-element compatibility) were qualities worth preserving. To this end, efforts were made toward improving and generalizing the existing element formulations to apply to arbitrary element shapes – polygons and polyhedra. Rather than relying upon shape functions defined through an isoparametric transformation from a parent element domain, recent polytopal element methodologies have explored various techniques for constructing approximants directly on the physical element domains. In doing so, issues regarding distorsion sensitivity of the elements are largely obviated, and new opportunities for discretizing the domain with irregular shapes are made possible.

In light of these developments, recent advances in meshing technologies have made polyhedral element methods a more readily feasible option. Very recently, Ebeida et. al. have released the software VoroCrust ([13]): an automated voronoi discretization tool

based on a constrained Poisson disk sampling methodology. Additionally, the Celeris CAE tool currently in development provides a means of intersecting a background graded hexahedral mesh with a piece-wise linear boundary representation (B-rep) to obtain a volume-filling polyhedral mesh.

For these reasons, efficient and robust polyhedral element formulations are in high demand, leading to a proliferation of different approaches. A number of these methods are discussed in the following section.

1.2 Recent Developments in Polytopal Discretizations

Polytopal element methods combine many of the attractive features of FEM with the geometric flexibility of having arbitrary element shapes, the primary motivation for which arises from the aforementioned concerns over discretization sensitivity. Many such methods share a few distinguishing features in common with one another: mesh degrees of freedom are borne by nodes – the geometric verticies of (low-order) elements; nodal basis functions are compactly supported over adjoining element domains, and satisfy the kronecker delta property; basis functions are defined directly on the element's physical domain, rather than on a parent domain.

Where these methods differ is in the way that they choose to define an element's shape functions, if at all. These approaches may be loosely categorized into three separate strategies: an explicit definition of the element's basis functions via a continuous interpolation scheme; an implicit definition of the element's shape functions via the Virtual Element Method (VEM); or a discrete representation of the element's shape functions via an approximation scheme. These three methodologies are elaborated upon in the following sections.

1.2.1 Continuous Interpolation on Arbitrary Polytopes

In an effort to generalize the core idea behind isoparametric element coordinates, which yield a point-wise definition of the element's shape functions and their gradients within a given element domain, various efforts to explicitly define shape functions directly on arbitrary polytopal domains has led to the creation of a broad family of interpolation

schemes, collectively referred to as *generalized barycentric coordinates*.

At a minimum, shape functions which fall into this category must: form a partition of unity, satisfy linear completeness, and interpolate the nodal data (i.e. satisfy the kronecker delta property). These coordinates are uniquely defined according to the standard barycentric coordinate system for simplicial domains. For arbitrary polytopal domains, numerous such coordinate systems exist, including Wachspress' coordinates [44], mean values coordinates [16], harmonic coordinates [20], and maximum entropy coordinates [39], among others.

Though generalized barycentric coordinates have been applied in the context of finite elements, their development has largely been propelled by the graphics community on account of their relatively smooth interpolatory properties. However, thier smooth (non-polynomial) character presents a challenge with regard to accurate numerical integration. Consequently, relatively high-order quadrature schemes are required to achieve reasonable accuracy and satisfaction of patch tests. More recently, a polynomial projection scheme has been suggested in [42] to remedy these integration errors for linear problems; for general nonlinear problems, a gradient correction scheme has been proposed in [43] and [8]. These developments have illuminated new possibilities for defining more efficient quadrature rules on polytopes while still satisfying the essential requirements for convergence.

Yet in spite of these developments, many existing coordinate schemes are sill limited by moderate to severe restrictions on element shape/convexity, and produce sharp gradients in the presence of degenerate geometric features. These concerns, and a recognition of the fact that the shape functions need not be defined point-wise for finite element applications, have motivated research efforts toward discrete representations of element interpolants.

1.2.2 Virtual Element Methods

The Virtual Element Method (VEM) summarized in [9] is a relatively new approach, and based in part upon the older concept of mimetic finite differences (MFD). Although the method supposes that continuous shape functions (trial and test functions) *exist* within arbitrary polytopal elements, the VEM never explicitly *defines* how these shape functions

vary on element interiors. Instead, the VEM supposes that these "virtual" functions may be separated (via projection operators) into polynomial and non-polynomial parts, which are handled in different ways.

The cornerstone of the method is the idea that the bilinear form for a given element may be decomposed into two distinct parts: a term which guarantees variational consistency (Galerkin exactness) involving the low-order polynomial part of the shape functions, and a term which provides stability involving the non-polynomial part. The consistency term must be integrated exactly, but the stability term can be evaluated approximately. Because this decomposition relies upon the linearity of the bilinear form, direct generalizations of the method to nonlinear problems are not immediately available.

VEM has been applied to three-dimensional elasticity problems in [17], though limited to strictly linear deformations and material behavior. In [10], a VEM formulation for low-order elements which accomodates nonlinear "black-box" constitutive algorithms is presented, and in [7] an extension to finite deformations (with appropriate stabilization terms) is introduced. Given the means by which these approaches exploit the use of a projected uniform gradient to integrate the stress divergence term, however, it is unclear how they could be extended to accomodate higher-order elements.

VEM formulations are able to tolerate geometric degeneracies and element non-convexity without encountering serious numerical difficulties, though their good behavior in the presence of these features is often governed by an ad hoc approximation of the stabilization terms. For this reason, it appears worthwhile to explore a more rigorous means of establishing the necessary stability requirements on more complicated element domains, while attempting to maintain the relative simplicity of the VEM.

1.2.3 Approximate Interpolation on Arbitrary Polytopes

Rather than defining shape functions either entirely explicitly, or implicitly, yet another strategy considers the representation of the element's shape functions in an approximate way, while enforcing a few essential requirements. Namely: polynomial reproducibility, inter-element compatibility, and consistency with the weak form.

In [29] and [31], Rashid and co-workers explored the variable element topology finite

element method (VETFEM), characterized by an approximate representation of the element's shape functions as low-order polynomials satisfying weak continuity requirements at element boundaries. Within this framework, the element shape functions are determined by a local minimization problem, selecting from a discrete approximation space of polynomials those shape functions which optimize specified continuity and smoothness objectives. This minimization procedure is constrained by the requirements of consistency and reproducibility to guarantee satisfaction of linear patch tests. Dohrmann and Rashid later extended this approach to higher-order elements in [12], instead focusing on a direct construction of the shape function derivatives, rather than of the shape functions themselves.

The VETFEM may be viewed as a non-conforming finite element method, as the minimization process altogether allows for residual discontinuities at inter-element boundaries. Nonetheless, because the elements satisfy weak contunity requirements, the method exhibits proper convergence characteristics. Additionally, because the VETFEM yields a point-wise representation of the shape functions as low-order polynomials, direct integration of the weak form can be carried out using relatively efficient domain quadrature rules.

Though the VETFEM was developed to handle arbitrary polygonal elements, it was observed to suffer from sensitivity to geometric degeneracies and element non-convexity. In response to these issues, a discrete data polyhedral finite element method (DDPFEM) proposed in [33] was suggested to exploit the fact that for typical solid mechanics applications, it is generally only necessary to evaluate the element's shape functions (and their derivatives) at a discrete number of quadrature points. The proposed method shares several characteristics in common with the VETFEM, utilizing a similarly posed constrained minimization procedure to obtain the precise values and gradients of the shape functions at discrete points on the element's interior. One of the cited challenges with this approach pertains to the appropriate selection of an efficient quadrature rule for the elements.

Nonetheless, the initial thoughts put forward by the DDPFEM ultimately led to the development of the partitioned element method (PEM) presented in [30]. The method

proceeds by partitioning an element into polygonal quadrature cells, and allowing the element's shape functions to vary according to a local polynomial defined within each of these cells, resulting in piece-wise polynomial shape functions which are discontinuous at quadrature cell boundaries. The polynomial coefficients defined in each cell are obtained by minimizing the discontinuities in the shape functions (and their gradients) across all cell interfaces, subject to the necessary consistency and reproducibility constraints. The original presentation in [30] considers the shape functions to be approximate solutions of Laplace's equation on the partitioned cell grid. Later developments have dispensed with the Laplacian term, instead penalizing discontinuities in shape function gradients at cell boundaries.

Subsequently, Bishop has proposed a similar partitioned element scheme in [4], wherein the elements and their faces are subdivided into simplicies, resembling a local FE discretization of the element domain. The shape functions are obtained as the solution to Laplace's equation on this subdivision. Because this approach utilizes an FE-like discretization, the resulting shape functions are piece-wise linear and C^0 continuous, thereby avoiding the need for a penalty term to enforce continuity. However, the method still requires the use of a gradient correction scheme to account for quadrature error and recover consistency.

Following these developments, we choose to recognize a new class of methods, herein collectively referred to as *partitioned element methods*. These may be viewed as a generalization of the original PEM presented in [30]. It is the subject of this thesis to further explore these methods, and to expose their particular merits and potential shortcomings.

1.3 Scope of the Present Work

In this work, we put forth a general framework for partitioned element methods as a collection of different approaches for constructing approximate representations of element shape functions on arbitrary polytopes. These methods share several features in common:

(1) Elements are discretized (partitioned) into non-overlapping polygonal cells. These cells are used to inform the quadrature rule of the element.

(2) A local approximation space is defined on the partitioned element geometry.

(3) A set of BVPs and appropriate constraints are posed, whose solutions yield the shape functions of the element.

(4) A stable numerical scheme is developed to obtain approximate solutions to these BVPs using the approximation space defined in (2).

Numerous formulations are possible within this framework; a few of these are explored within the scope of this thesis.

The application area of interest for these methods is in nonlinear solid mechanics. The efficacy of the methods explored will be assessed within this context, with regard to their ability to naturally accomodate nonlinear kinematic and material behavior. The robustness of the resulting elements, and their performance in the face of locking phenomena will be evaluated. Additionally, several methodologies which leverage the partitioned element framework to combat certain forms of locking will be discussed.

The remainder of this dissertation is organized as follows: Chapter 2 establishes the context of nonlinear computational solid mechanics. Chapter 3 presents the overarching framework for partitioned element methods. Chapter 4 details a particular implementational framework for the PEM. Chapter 5 provides a number of numerical investigations of the PEM. Chapter 6 concludes with a discussion of opportunities for further research and development.

Chapter 2

An Overview of Computational Solid Mechanics

This chapter addresess some of the essential aspects of numerical approximation methods for modeling solid continua. The discussion herein will focus on the mathematical foundations of solid mechanics, beginning with the kinematics of motion and some common forms of constitutive relationships, followed by the expressions for conservation of momentum in both strong and weak form, and concluding with an analysis of the standard numerical methods utilized to solve these equations in an approximate sense. In the course of our discussion, we will make explicit the ensuing requirements placed upon any prospective approximation scheme. This will aid our analysis in subsequent chapters, and hopefully justify particular choices made in the construction of partitioned element methods.

2.1 The Lagrangian Description of Motion

Consider a body $\Omega_0 \subset \mathbb{R}^d$ consisting of a set of material points whose positions in some reference configuration at time $t = 0$ are denoted $\mathbf{X}$. At a later time $t > 0$, the body occupies a new configuration $\Omega_t = \chi(\Omega_0, t) \subset \mathbb{R}^d$, such that the motion of individual material points yield new spatial positions $\mathbf{x}$ according to the bijection $\chi_t : \mathbf{X} \leftrightarrow \mathbf{x}$, i.e.

$$\mathbf{x} = \chi(\mathbf{X}, t), \quad \mathbf{X} = \chi^{-1}(\mathbf{x}, t). \tag{2.1}$$

The displacement $\mathbf{u}$ of a given material point may be expressed as $\mathbf{u} = \mathbf{x} - \mathbf{X}$, and it's corresponding velocity is denoted $\mathbf{v} = \dot{\mathbf{x}} = \partial\mathbf{x}/\partial t$. Figure 2.1 provides a visual interpretation of the situation described.

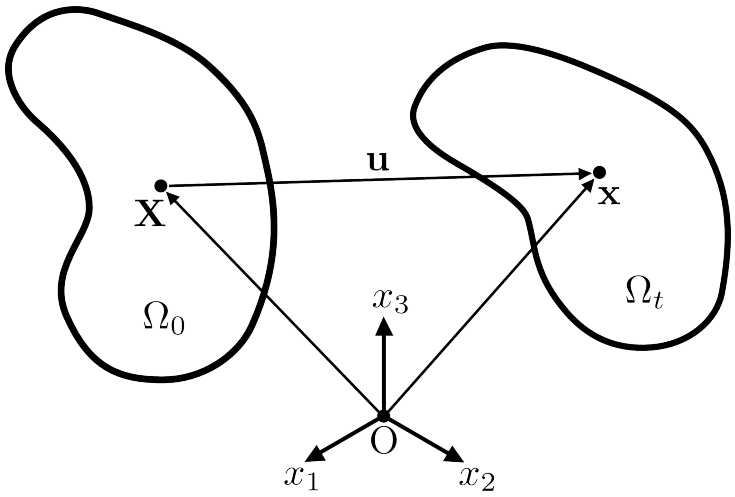

Figure 2.1. A depiction of the motion of material points in a body Ω.

At a given time t, the Jacobian of the deformation mapping χ_t yields the deformation gradient $\mathbf{F} = \nabla_X \mathbf{x}$ (a rank-2 tensor), defined as

$$\mathbf{F} = \frac{\partial \mathbf{x}}{\partial \mathbf{X}} = \mathbf{1} + \nabla_X \mathbf{u}, \tag{2.2}$$

where ∇_X denotes the gradient with respect to $\mathbf{X}$. The deformation gradient may be used to map differential line segments $d\mathbf{X}$, surface areas $d\mathbf{A}$, and volumes dV defined in the reference configuration into their corresponding transformed quantities ($d\mathbf{x}$, $d\mathbf{a}$, dv) at time t:

$$d\mathbf{x} = \mathbf{F} d\mathbf{X} \tag{2.3}$$

$$d\mathbf{a} = J\mathbf{F}^{-T}d\mathbf{A} \tag{2.4}$$

$$dv = JdV \tag{2.5}$$

where $J \equiv \det \mathbf{F}$.

In a similar fashion, the spatial velocity gradient $\mathbf{L} = \nabla_x \mathbf{v}$ (where ∇_x denotes the gradient with respect to $\mathbf{x}$) may be expressed as

$$\mathbf{L} = \frac{\partial \mathbf{v}}{\partial \mathbf{x}} = \frac{\partial \dot{\mathbf{x}}}{\partial \mathbf{X}} \frac{\partial \mathbf{X}}{\partial \mathbf{x}} = \dot{\mathbf{F}}\mathbf{F}^{-1}, \tag{2.6}$$

which may be further decomposed into a symmetric part $\mathbf{D}$ (the rate of deformation tensor) and an anti-symmetric part $\mathbf{W}$ (the spin tensor):

$$\mathbf{D} = \frac{1}{2}(\mathbf{L} + \mathbf{L}^T), \quad \mathbf{W} = \frac{1}{2}(\mathbf{L} - \mathbf{L}^T). \tag{2.7}$$

2.1.1 Compatibility

In continuum mechanics, compatibility refers to the idea that a given body remains a contiguous medium following some deformation described by χ_t. In other words, χ_t must characterize a continuous mapping of material points between different configurations in time, such that the topology of body remains unchanged. Compatibilitiy is characterized by the following necessary and sufficient conditions:

$$\nabla_X \times \mathbf{F} = \mathbf{0}. \tag{2.8}$$

Satisfaction of the above compatibility condition implies that there exists a continuous, single-valued displacement field which gives rise to the deformation characterized by $\mathbf{F}$.

2.1.2 Finite Strain Measures

Consider the set of all material line segments $d\mathbf{X}$ which lie in a small neighborhood around a given material point $\mathbf{X}$. Also, consider these same material line segments $d\mathbf{x}$ in the current configuration of the body after some deformation corresponding to $\mathbf{F}(\mathbf{X}, t)$ has taken place, such that $d\mathbf{x} = \mathbf{F}d\mathbf{X}$.

At a given material point $\mathbf{X}$, the deformation gradient $\mathbf{F}(\mathbf{X}, t)$ may be characterized as a linear operator, which may be decomposed into two step-wise operations: a stretching

operation $\mathbf{U}$ (or $\mathbf{V}$), and a rotation $\mathbf{R}$, yielding the polar decomposition of $\mathbf{F}$:

$$\mathbf{F} = \mathbf{RU} = \mathbf{VR}, \tag{2.9}$$

where $\mathbf{U}$ is termed the right stretch tensor, and $\mathbf{V}$ is the left stretch tensor. There arise from $\mathbf{U}$ and $\mathbf{V}$ two primary deformation measures: the right Cauchy-Green deformation tensor $\mathbf{C} = \mathbf{U}^2$, and the left Cauchy-Green deformation tensor $\mathbf{B} = \mathbf{V}^2$. Each of these, in turn, yield two of the most commonly utilized finite strain measures: the Green-Lagrangian strain tensor $\mathbf{E} = \frac{1}{2}(\mathbf{C} - \mathbf{I})$, and the Eulerian-Almansi strain tensor $\mathbf{e} = \frac{1}{2}(\mathbf{I} - \mathbf{B}^{-1})$. It is not difficult to show that both of these strain measures reduce to the small strain tensor $\boldsymbol{\varepsilon} = \frac{1}{2}(\nabla_X \mathbf{u} + (\nabla_X \mathbf{u})^T)$ if the displacements are sufficiently small.

Another finite strain measure that has gained attention in more recent years is the Hencky (logarithmic, or "true") strain tensor $\mathbf{H} = \frac{1}{2}\log \mathbf{B}$. Because the Hencky strain tensor belongs to the Seth-Hill family of strain measures (as do the Green-Lagrangian and Eulerian-Almansi strain tensors), it likewise is seen to reduce to the small strain tensor in the limit of small displacements.

2.2 Conservation of Linear and Angular Momentum

For a given material body $\mathcal{B}_t \subset \mathbb{R}^d$, any open subset $\Omega_t \subset \mathcal{B}_t$ must satisfy Newton's second law of motion, such that the net external force which acts upon Ω_t is equal to the total change in linear momentum of the system, i.e.

$$\frac{d}{dt}\int_{\Omega_t} \rho \mathbf{v}\, dv = \int_{\Omega_t} \rho \mathbf{b}\, dv + \int_{\partial\Omega_t} \mathbf{t}\, da \quad \forall \Omega_t \subset \mathcal{B}, \tag{2.10}$$

where ρ is the mass density of the matertial, $\mathbf{v}$ is the velocity field, $\mathbf{b}$ is an applied body force per unit of mass, and $\mathbf{t}$ is the traction vector – a force per unit of area – which acts on $\partial\Omega_t$ (the boundary of Ω_t). Via the Cauchy tetrahedron argument, it is possible to express the traction vector $\mathbf{t}(\mathbf{n})$ as a linear function of the unit vector $\mathbf{n}$, which is normal to the surface upon which the traction acts:

$$\mathbf{t} = \mathbf{n} \cdot \boldsymbol{\sigma}, \tag{2.11}$$

where $\boldsymbol{\sigma}$ is referred to as the Cauchy stress tensor. Invoking the divergence theorem, we may utilize the above relation to convert the traction boundary integral into a volume

integral over Ω_t:

$$\int_{\partial\Omega_t} \mathbf{t}\, da = \int_{\partial\Omega_t} \mathbf{n}\cdot\boldsymbol{\sigma}\, da = \int_{\Omega_t} \nabla_x\cdot\boldsymbol{\sigma}\, dv. \tag{2.12}$$

Moreover, utilizing Reynolds' transport theorem, conservation of mass, and a change of variables in $\mathbf{x}$ and $\mathbf{X}$, it is possible to show that

$$\frac{d}{dt}\int_{\Omega_t} \rho\mathbf{v}\, dv = \int_{\Omega_t} \rho\frac{d\mathbf{v}}{dt}\, dv, \tag{2.13}$$

which ultimately yields

$$\int_{\Omega_t} \left[\rho(\mathbf{b}-\dot{\mathbf{v}}) + \nabla_x\cdot\boldsymbol{\sigma}\right] dv = \mathbf{0} \quad \forall\Omega_t \subset \mathcal{B}. \tag{2.14}$$

Since we have imposed no limitations on the choice of subset Ω_t, we may invoke the localization theorem to determine a point-wise statement of equilibrium in the body $\mathcal{B}_t$:

$$\rho(\mathbf{b}-\dot{\mathbf{v}}) + \nabla_x\cdot\boldsymbol{\sigma} = \mathbf{0} \quad \forall\mathbf{x}\in\mathcal{B}_t. \tag{2.15}$$

Similarly, by formulating an expression for the conservation of angular momentum and following an analogous procedure, we obtain an additional point-wise requirement on the symmetry of the Cauchy stress tensor:

$$\boldsymbol{\sigma} = \boldsymbol{\sigma}^T \quad \forall\mathbf{x}\in\mathcal{B}_t. \tag{2.16}$$

2.2.1 Measures of Stress

As expressed earlier, the Cauchy stress tensor $\boldsymbol{\sigma}$ relates the normal $\mathbf{n}$ of a given surface area element $d\mathbf{a} = \mathbf{n}\, da$ to the corresponding force per unit of area $\mathbf{t}$ which acts on that surface, where the surface element $d\mathbf{a}$ is defined in the current configuration of the body (at some time $t > 0$). The total force which acts on a given surface $d\mathbf{a}$ is then

$$d\mathbf{f} = \mathbf{t}\, da = \boldsymbol{\sigma}^T\, d\mathbf{a}. \tag{2.17}$$

Utilizing Nanson's formula for area transformations:

$$d\mathbf{a} = J\mathbf{F}^{-T}\, d\mathbf{A}, \tag{2.18}$$

we may consider an equivalent representation of $d\mathbf{f}$, such that

$$d\mathbf{f} = J\boldsymbol{\sigma}^T\mathbf{F}^{-T}\, d\mathbf{A} = \mathbf{P}\, d\mathbf{A} = \mathbf{p}\, dA, \tag{2.19}$$

where $\mathbf{P}$ is defined as the first Piola-Kirchhoff stress tensor (which in general is not symmetric.), and where $\mathbf{p} = \mathbf{N} \cdot \mathbf{P}^T$ is the corresponding Piola traction vector, characterizing the distributed force which acts over a surface defined in the reference configuration with area dA and normal $\mathbf{N}$.

Another stress measure (related to the first Piola-Kirchhoff stress) is the second Piola-Kirchhoff stress tensor $\mathbf{S}$, which is commonly defined as the pull-back of the Kirchhoff stress tensor $\boldsymbol{\tau} = J\boldsymbol{\sigma}$:

$$\mathbf{S} = \mathbf{F}^{-1}\boldsymbol{\tau}\mathbf{F}^{-T}. \tag{2.20}$$

2.3 Constitutive Relations

Fundamentally, we require there to be some relationship between the forces applied to a given body, and the observed deformation of those bodies. Such relationships are generally referred to as constitutive models, which characterize a macroscopic connection between stress and strain in a continuum.

2.3.1 Models of Elasticity

Constitutive models have variable forms, mostly notably as they relate to notions of elasticity: the tendency of a material to revert to its original undeformed configuration if the applied forces are removed. Models for elastic material behavior fall into three primary categories: hyperelasticity, Cauchy-elasticity, and hypoelasticity.

Hyperelasticity is concerned with the description of a material's state through an elastic potential function, which characterizes the total stored elastic strain energy $W(\mathbf{F})$ in the material as a function of the total deformation measured from some (nominally undeformed) reference configuration. Differentiation of this potential with respect to a given deformation measure will yield an expression for the corresponding work-conjugate measure of stress, e.g.

$$\mathbf{P} = \frac{\partial W}{\partial \mathbf{F}}, \qquad \mathbf{S} = \frac{\partial W}{\partial \mathbf{E}}. \tag{2.21}$$

Some common examples of hyperelastic models include the St. Venant-Kirchhoff material model:

$$W(\mathbf{E}) = \frac{\lambda}{2}\mathrm{tr}(\mathbf{E})^2 + \mu\mathrm{tr}(\mathbf{E}^2), \tag{2.22}$$

Hencky's elasticity model:

$$W(\mathbf{H}) = \frac{\lambda}{2}\mathrm{tr}(\mathbf{H})^2 + \mu\mathrm{tr}(\mathbf{H}^2), \tag{2.23}$$

the compressible Mooney-Rivlin solid:

$$W(I_1, I_2, J) = C_{01}(J^{-4/3}I_2 - 3) + C_{10}(J^{-2/3}I_1 - 3) + D_1(J-1)^2, \tag{2.24}$$

$$I_1 = \mathrm{tr}(\mathbf{B}), \qquad I_2 = \frac{1}{2}\left[\mathrm{tr}(\mathbf{B})^2 - \mathrm{tr}(\mathbf{B}^2)\right], \qquad J = \det(\mathbf{F}), \tag{2.25}$$

$$D_1 = \frac{\kappa}{2}, \qquad (C_{01} + C_{10}) = \frac{\mu}{2}, \tag{2.26}$$

and the compressible Neo-Hookean solid (a special case of the Mooney-Rivlin solid where $C_{01} = 0$, and $C_1 = C_{10}$):

$$W(I_1, J) = C_1(J^{-2/3}I_1 - 3) + D_1(J-1)^2 \tag{2.27}$$

Cauchy-elasticity (as a terminology to describe a particular sub-class of material models) differs from hyperelasticity in the sense that the relations between particular stress and strain measures are defined directly, and do not necessarily arise from an elastic potential function. The models of linear elasticity, in particular, are generalizations of Hooke's law, namely:

$$\boldsymbol{\sigma} = \mathbf{C} : \boldsymbol{\varepsilon}, \tag{2.28}$$

and are suitable for small deformations, but are typically not applicable in the context of finite deformations. By comparison, Cauchy-elastic models are defined in terms of the deformation gradient $\mathbf{F}$, i.e.

$$\boldsymbol{\sigma} = f(\mathbf{F}), \tag{2.29}$$

and are more suitable in the realm of finite deformations. For such models to be considered objective under a superposed rigid rotation corresponding to $\mathbf{R}$, they must satisfy the following condition:

$$\mathbf{R}\boldsymbol{\sigma}\mathbf{R}^T = f(\mathbf{RF}). \tag{2.30}$$

Nonetheless, such models may still suffer from being non-conservative, in the sense that the total work done by the stresses in moving through an arbitrary closed cycle of deformation

does not necessarily sum to zero. For these reasons, models of hyperelasticity are generally preferred where the use of such models is deemed appropriate. Nonetheless elasticity models are still useful, particularly in the context of small deformations.

In contrast, hypoelasticity models define an evolution (rate) equation in terms of the current stress and the velocity gradient at a given material point, i.e.

$$\dot{\boldsymbol{\sigma}} = g(\boldsymbol{\sigma}, \mathbf{L}). \tag{2.31}$$

Hypoelasticity models are in general non-conservative, and moreover may not necessarily return to a state of zero stress following a closed cycle of deformation. Hypoelasticity is generally less appropriate where hyperelastic or other elastic models may be used instead. The value of hypoelasticity lies in its ability to accomodate models for plastic flow and dissipation in the material, giving rise to the common models of hypoelasto-plasticity.

One of the primary challenges of working with hypoelastic models concerns the manner in which the rate of stress transforms under superposed rigid-body rotations. These considerations have led to the formulation of co-rotational (or objective) stress rates. A multitude of such rates exist, though only a few are found to be in common usage. Most notably, the Jaumann rate of stress $\mathring{\boldsymbol{\sigma}}$ is defined as

$$\mathring{\boldsymbol{\sigma}} = g(\boldsymbol{\sigma}, \mathbf{D}) = \dot{\boldsymbol{\sigma}} + \boldsymbol{\sigma}\mathbf{W} - \mathbf{W}\boldsymbol{\sigma}, \tag{2.32}$$

where $\mathbf{D}$ and $\mathbf{W}$ specify the rate of deformation and spin at a given material point, respectively.

2.3.2 Equations of Material State

In a continuum body $\mathcal{B}_t$, every material point $\mathbf{x} \in \mathcal{B}_t$ is endowed with a "material state" $S_t(\mathbf{x})$ at time t. In the context of Lagrangian solid mechanics, the material state $S_t = \{\boldsymbol{\sigma}, q_*\}$ typically consists of the Cauchy stress tensor $\boldsymbol{\sigma}$, and any (possibly tensorial) internal state variables q_* associated with the material model.

In a computational setting, the analysis is usually subdivided into discrete time steps $\{t_k\}_{k=0}^{N}$, and the motion of material points from time t_k to t_{k+1} is described by an incremental displacement field, denoted $\hat{\mathbf{u}} = \mathbf{u}_{k+1} - \mathbf{u}_k$. The deformation associated with this

motion may be characterized by an incremental deformation gradient $\hat{\mathbf{F}} = \partial \mathbf{x}_{k+1} / \partial \mathbf{x}_k = \mathbf{1} + \nabla_{x_k} \hat{\mathbf{u}}$.

Assuming that the material behaves in a rate-independent manner, a generic constitutive model $f \colon (S_k, \nabla_{x_k} \hat{\mathbf{u}}) \mapsto S_{k+1}$ should yield the updated material state S_{k+1} at time t_{k+1} as a function of the material state S_k at time t_k, and the incremental displacement gradient $\nabla_{x_k} \hat{\mathbf{u}}$.

2.4 A Model Solid Mechanics Boundary Value Problem

Up to this point, we have discussed only the essential relationships which exist between physical quantities of interest in the context of solid mechanics. Ultimately, however, we should like to determine the anticipated motion and deformation of a particular body under the action of pre-determined externally applied forces. To this end, we must turn our attention to the definition – and solution – of a corresponding boundary value problem (BVP). Such problems must be well-posed, in the sense that there exists a unique solution to the stated problem, thereby imposing certain restrictions on the choice of boundary conditions.

2.4.1 The Strong Form Statement of Equilibrium

In the context of solid mechanics, the solution of a given boundary value problem usually refers to a complete description of the primary field variable(s) of interest, namely the displacement field $\mathbf{u}(\mathbf{X})$ at all locations $\mathbf{X} \in \mathcal{B}_0$ within the body $\mathcal{B}_0$ in its reference configuration. Under the requirements of compatibility, we presume that the displacement field is a continuous function, whose derivatives up to second order are defined everywhere, i.e. $\mathbf{u} \in [C^2(\mathcal{B}_0)]^d$.

Now, let us examine a quasi-static solid mechanics model problem of the following form: consider an open domain $\mathcal{B}_0 \subset \mathbb{R}^d$ whose boundary $\partial \mathcal{B}_0$ consists of the partition $\{\Gamma_u, \Gamma_t\}$. Let $\mathbf{u} = \bar{\mathbf{u}}\ \forall \mathbf{X} \in \Gamma_u$ constitute a prescribed Dirichlet boundary condition imposed upon the displacement field, and $\mathbf{n} \cdot \boldsymbol{\sigma} = \bar{\mathbf{t}}\ \forall \mathbf{X} \in \Gamma_t$ be a Neumann boundary condition imposed upon the surface traction. Additionally, let us suppose that an applied

body force $\mathbf{b}$ acts upon all points $\mathbf{X} \in \mathcal{B}_0$. Given these conditions, we should like to determine the displacement field $\mathbf{u} \in \mathcal{S} = \left\{ \mathbf{u} \in [C^2(\mathcal{B}_0)]^d : \mathbf{u} = \bar{\mathbf{u}} \ \forall \mathbf{x} \in \Gamma_u \right\}$ which satisfies the equations of equilibrium in a point-wise sense:

$$\rho \mathbf{b} + \nabla_x \cdot \boldsymbol{\sigma} = \mathbf{0} \quad \forall \mathbf{x} \in \mathcal{B}_t, \tag{2.33}$$

and where we suppose that a constitutive model has been defined in order to relate some measure of the deformation (e.g. $\mathbf{F} = \mathbf{1} + \nabla_X \mathbf{u}$) to the stress (e.g. $\boldsymbol{\sigma} = f(\mathbf{F})$). Equivalently, we may write the equations of equilibrium in terms of quantities related to the reference configuration of the body:

$$\rho_0 \mathbf{b} + \nabla_X \cdot \mathbf{P}^T = \mathbf{0} \quad \forall \mathbf{X} \in \mathcal{B}_0, \tag{2.34}$$

where $\rho_0 = J\rho$ is the mass density of the material at time $t = 0$. The above statement is commonly referred to as the "strong form" of the model problem, given that it requires a point-wise satisfaction of equilibrium.

It should be emphasized that the Dirichlet boundary conditions and the requirements of compatibility are satisfied implicitly, as a consequence of the deliberate choice of function space $\mathcal{S}$ for the displacement field. Such functions $\mathbf{u} \in \mathcal{S}$ are termed "admissible," as potential solutions to the boundary value problem at hand.

2.4.2 The Equivalent Weak Form Statement of Equilibrium

In general, solutions to the strong form problem are not easily obtained. For this reason, it proves to be much more convenient to work with the (equivalent) "weak form" statement of the boundary value problem:

Find $\mathbf{u} \in \mathcal{S} = \left\{ \mathbf{u} \in [H^1(\mathcal{B}_0)]^d : \mathbf{u} = \bar{\mathbf{u}} \ \forall \mathbf{X} \in \Gamma_u \right\}$ *such that*

$$\int_{\chi(\mathcal{B}_0,t)} \rho \mathbf{b} \cdot \mathbf{v} \, dv + \int_{\chi(\Gamma_t,t)} \bar{\mathbf{t}} \cdot \mathbf{v} \, da - \int_{\chi(\mathcal{B}_0,t)} \boldsymbol{\sigma} \colon \nabla_x \mathbf{v} \, dv = 0 \quad \forall \mathbf{v} \in \mathcal{V}, \tag{2.35}$$

or equivalently

$$\int_{\mathcal{B}_0} \rho_0 \mathbf{b} \cdot \mathbf{v} \, dV + \int_{\Gamma_t} \bar{\mathbf{p}} \cdot \mathbf{v} \, dA - \int_{\mathcal{B}_0} \mathbf{P} \colon \nabla_X \mathbf{v} \, dV = 0 \quad \forall \mathbf{v} \in \mathcal{V}, \tag{2.36}$$

where $\mathcal{V} = \left\{ \mathbf{v} \in [H^1(\mathcal{B}_0)]^d : \mathbf{v} = \mathbf{0} \ \forall \mathbf{X} \in \Gamma_u \right\}$, *and*

$$H^1(\mathcal{B}_0) = \left\{ u \in L^2(\mathcal{B}_0), \, D^\alpha u \in L^2(\mathcal{B}_0) \ \forall |\alpha| \leq 1 \right\}. \tag{2.37}$$

In (2.36), the traction boundary condition has been replaced by $\mathbf{p} = \bar{\mathbf{p}}\ \forall \mathbf{X} \in \Gamma_t$ – i.e. a condition on the Piola (rather than Cauchy) surface traction. The function space $\mathcal{S}$ is commonly referred to as the space of admissible "trial solutions," whereas $\mathcal{V}$ is called the space of "test functions," and consists of all admissible variations such that $\mathcal{V} = T_{\mathbf{u}}\mathcal{S}$ is the tangent space to $\mathcal{S}$ (i.e. $\mathbf{u} + \mathbf{v} \in \mathcal{S}\ \forall \mathbf{u} \in \mathcal{S}$, $\mathbf{v} \in \mathcal{V}$). In words, our goal is determine the solution $\mathbf{u}$ from among all admissible trial solutions contained in $\mathcal{S}$ which satisfies equation (2.35) or (2.36) for all admissible variations $\mathbf{v} \in \mathcal{V}$.

Under the assumptions of small displacements and linear elasticity, equations (2.35) and (2.36) are equivalent, and may be more succinctly expressed in terms of a bilinear form $a(\cdot,\cdot)\colon \mathcal{S} \times \mathcal{V} \mapsto \mathbb{R}$ and a linear form $\ell(\cdot) : \mathcal{V} \mapsto \mathbb{R}$ such that

$$a(\mathbf{u}, \mathbf{v}) + \ell(\mathbf{v}) = 0 \quad \forall \mathbf{v} \in \mathcal{V}. \tag{2.38}$$

2.5 Galerkin Approximations to the Weak Form

In the weak form problem statement, the trial and test spaces $\mathcal{S}$ and $\mathcal{V}$ are taken to be infinite dimensional function spaces. In a practical computational setting, however, this renders the solution of such problems infeasible. Instead, most variational methods consider approximate solutions to the weak form, where $\mathbf{u} \in \mathcal{S}$ and $\mathbf{v} \in \mathcal{V}$ are replaced by $\mathbf{u}^h \in \mathcal{S}^h \subset \mathcal{S}$ and $\mathbf{v}^h \in \mathcal{V}^h \subset \mathcal{V}$, respectively. In this context, $\mathcal{S}^h = \{\varphi_a\}_{a=1}^N$ and $\mathcal{V}^h = \{\phi_a\}_{a=1}^M$ denote finite dimensional sub-spaces of $\mathcal{S}$ and $\mathcal{V}$, such that

$$\mathbf{u}^h = \sum_{a=1}^{N} \varphi_a \mathbf{u}_a, \qquad \mathbf{v}^h = \sum_{a=1}^{M} \phi_a \mathbf{v}_a. \tag{2.39}$$

This yields the Galerkin approximation to the weak form: *Find* $\mathbf{u}^h \in \mathcal{S}^h$ *such that*

$$\int_{\mathcal{B}_t} \rho \mathbf{b} \cdot \mathbf{v}^h \, dv + \int_{\chi_{(\Gamma_t,t)}} \bar{\mathbf{t}} \cdot \mathbf{v}^h \, da - \int_{\mathcal{B}_t} \boldsymbol{\sigma} \colon \nabla_x \mathbf{v}^h \, dv = 0 \quad \forall \mathbf{v}^h \in \mathcal{V}^h, \tag{2.40}$$

or equivalently

$$\int_{\mathcal{B}_0} \rho_0 \mathbf{b} \cdot \mathbf{v}^h \, dV + \int_{\Gamma_t} \bar{\mathbf{p}} \cdot \mathbf{v}^h \, dA - \int_{\mathcal{B}_0} \mathbf{P} \colon \nabla_X \mathbf{v}^h \, dV = 0 \quad \forall \mathbf{v}^h \in \mathcal{V}^h. \tag{2.41}$$

Without loss of generality, if we suppose that $\mathcal{S} = \mathcal{V}$ (provided $\mathbf{u} = \mathbf{0}\ \forall \mathbf{X} \in \Gamma_u$), then we may select identical sub-spaces $\mathcal{S}^h = \mathcal{V}^h = \{\varphi_a\}_{a=1}^N$, resulting in a symmetric

(or Bubnov-) Galerkin method. Traditional finite element methods fall into this category. Such methods are advantageous in the sense that (for linear problems) they result in stable, symmetric bilinear forms satisfying the Galerkin orthgonality (or "best approximation") property – the property that the solution error $\mathbf{e} = \mathbf{u}^h - \mathbf{u}$ is orthogonal to the chosen sub-space $\mathcal{S}^h$. This is a direct consequence of $\mathcal{V}^h = T_{\mathbf{u}^h}\mathcal{S}^h$ (i.e. $\mathbf{u}^h + \mathbf{v}^h \in \mathcal{S}^h \; \forall \mathbf{u}^h \in \mathcal{S}^h$, $\mathbf{v}^h \in \mathcal{V}^h$).

Petrov-Galerkin methods consider the more general case where $\mathcal{V}^h \neq \mathcal{S}^h$, resulting in differing trial and test function spaces. Such methods must guarantee satisfaction of the LBB (inf-sup) conditions to achieve convergence. Consequently, the selection of appropriate trial and test function spaces which result in stable discretizations is not trivial. Nonetheless, Petrov-Galerkin methods allow for greater flexibility in the construction of numerical approximation schemes.

2.5.1 Finite Element Methods

Finite element methods (FEM) are predicated on the idea that a problem domain $\mathcal{B}$ can be discretized into a finite number of simpler sub-domains $\omega_e \subset \mathcal{B}$, individually called elements, and collectively referred to as a "mesh." The basis functions are assumed to be low-order polynomials within each element which possess compact support over a given patch of elements. The traditional finite element method assumes these basis functions to be C^0 continuous at element boundaries, yielding a priori satisfaction of compatibility.

Individual FE basis functions φ_a are typically associated with the "nodes" $\mathbf{X}_a$ of the mesh (located at element verticies, along element edges, etc.), such that the kronecker delta property is satisfied:

$$\mathbf{u}^h(\mathbf{X}_b) = \sum_{a=1}^{N} \varphi_a(\mathbf{X}_b)\mathbf{u}_a = \mathbf{u}_b. \tag{2.42}$$

Consequently, the basis functions comprise a set of interpolants for discrete values of the solution defined at the nodes.

Elements consisting of regular shapes (tetrahedra, hexahedra) also provide a natural means of effecting numerical integration of the weak form through the use of the isoparametric transformation and product Gaussian quadrature rules.

2.6 Requirements for Convergence of an Approximation Method

2.6.1 Satisfaction of Essential Boundary Conditions

2.6.2 Completeness/Approximability

2.6.3 Variational Consistency

2.6.3.1 Constraints on Numerical Quadrature

2.6.4 Numerical Stability

2.6.4.1 The Inf-Sup Condition

2.6.5 Tests for Convergence

2.6.5.1 The Irons Patch Test

2.6.5.2 The Generalized Patch Test

2.6.5.3 The F-E-M Test

2.7 Sources of Solution Nonlinearity in Solid Mechanics

2.7.1 Finite Deformations and Nonlinear Kinematics

2.7.2 Nonlinear Material Behavior

2.7.3 Requirements of the Approximation Method

Chapter 3

Partitioned Element Methods

This chapter defines a general class of polytopal element formulations, herein referred to as partitioned element methods (PEM). The essential mathematical requirements placed upon these methods are formally stated, giving rise to a family of different approaches, for which some formal investigations are conducted. Several specific formulations are summarized in detail, and a number of existing methods are herein classified as partitioned element methods.

3.1 Overview

A partitioned element method is a finite element-like method which approaches the task of constructing shape functions on an arbitrary element domain by partitioning the element into simpler sub-domains, and establishing a finite sub-space of approximating functions defined on this partition. Optimal shape functions are selected from this approximation space which minimize a chosen objective functional, while respecting any imposed constraints.

The rationale behind this paradigm stems from the idea that it is generally easier to define shape functions which preserve desirable characteristics over arbitrary polytopal domains if the shape functions are defined in a piece-wise polynomial fashion over simpler sub-domains.

Partitioned element methods encompass the special case where each element consists of a single sub-domain, thereby reducing the method to a VEM or VETFEM-like approach.

Such methods typically require more rigorous mesh regularity requirements be satisfied to obtain favorable results, however. These approaches are not particularly robust when applied to arbitrary polyhedral meshes, namely those generated by B-rep intersection, and they perform poorly if the element's geometry is sufficiently complicated.

At a minimum, the partitioned element method must satisfy 4 primary conditions:

- **Reproducibility**: The shape functions (and their derivatives) must be capable of exactly reproducing any polynomial field up to a specified order k.
- **Compatibility**: The shape functions must maintain a sufficient degree of continuity at inter-element and intra-element interfaces.
- **Stability**: The local bilinear form defined on the element must satisfy the inf-sup condition.
- **Consistency**: The element must exactly integrate the weak form equations when the solution corresponds to a polynomial of maximal degree k.

In the following sections, an abstract framework for the PEM is established, and the above conditions are made precise in mathematical terms.

3.2 An Abstract Partitioned Element Framework

3.2.1 The Element Partition

- Provide a figure of an element with partitioned geometry
- Define partitioned geometry terms (cells, facets, segments, verticies, etc.), perhaps even give a table of definitions, all referring back to the main figure(s)
-

3.2.2 Partition-Based Approximation Spaces

Traditional approximation methods typically consider the independent specification of two principal transformations: an interpolation scheme, which is necessary to represent

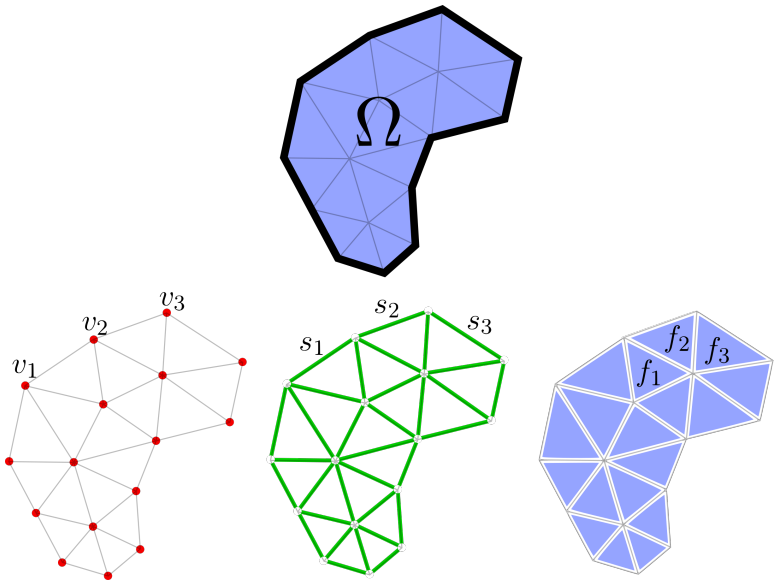

Figure 3.1. A representative domain $\Omega \subset \mathbb{R}^2$, and it's corresponding partition into verticies, segments, and facets.

field variables according to known point-values; and a quadrature rule, for the purposes of integrating such fields over the domain on which they are defined.

In mathematical terms, an interpolant φ is a linear operator which maps vectors $\mathbf{u} \in \mathbb{R}^k$ containing point-wise data regarding a field into scalar functions $f \in V^k(\Omega)$, i.e.

$$\varphi \colon \mathbb{R}^k \mapsto V^k(\Omega) \tag{3.1}$$

where $\mathbb{R}^k$ is a k-dimensional real space, and $V^k(\Omega)$ is a k-dimensional function space defined on Ω.

By constrast, a quadrature rule Σ is a linear operator which maps scalar functions $f \in V^k(\Omega)$ to vectors $\mathbf{q} \in \mathbb{R}^p$ identifying point-wise samples of f, i.e.

$$\Sigma \colon V^k(\Omega) \mapsto \mathbb{R}^p \tag{3.2}$$

The composition $\Sigma \circ \varphi$ of an interpolant φ with a quadrature rule Σ yields a linear operator

$$\Sigma \circ \varphi \colon \mathbb{R}^k \mapsto \mathbb{R}^p \tag{3.3}$$

3.2.3 Selection of an Appropriate Objective Functional

Once we have specified a given approximation space of functions, our goal is then to select the function from this space which best represents the nodal data that we are attempting

to interpolate over the element. The essential question is this: by what metric should we objectively assess the appropriateness of a given approximating function?

3.2.4 Construction of Element Appoximants

3.3 Essential Requirements of the PEM

3.3.1 Reproducibility

Fundamentally, the approximation power of the PEM depends directly upon the degree of completeness of the underlying approximation space. In particular, the finite-dimensional trial solution space $\mathcal{S}^h$ should contain as a subspace $\mathbb{P}_k \subset \mathcal{S}^h$ for some $k \geq 0$, where $\mathbb{P}_k$ denotes the subspace of polynomial functions with maximal degree k. This guarantees that the PEM approximation space will be capable of exactly reproducing any polynomial function up to some specified order.

3.3.1.1 Requirements of the Approximation Space

3.3.2 Compatibility

Compatibility, in an abstract sense, refers to the property of there being a unique displacement field (up to rigid translations) which gives rise to a particular strain field. This condition is satisfied directly if the displacement field is continuous (i.e. if the displacement field $\mathbf{u} \in C^0$). This condition is met if standard "compatible" finite elements are utilized, whose trial solution space $\mathcal{S}^h$ is a subset of C^0, namely $\mathcal{S}^h \subset H^1 \subset C^0$.

Failure to satisfy compatibility in a strong sense (i.e. point-wise) does not altogether preclude the convergence of a given approximation method. Some authors have proposed that satisfaction of the Irons patch test is sufficient for convergence. It was later shown, however, that the Irons patch test is neither sufficient, nor necessary for convergence. Most notably, Stummel has proposed in [37] the necessary and sufficient conditions for convergence of a non-conforming finite element method. These conditions include approximability, and passage of a so-called "generalized patch test," which asserts:

For a given patch $S \subset \overline{\Omega}$ and an approximating sequence of functions $u^h \in H^k(\Omega^h)$:

for every $\mathbf{x} \in S$ *there exists an open neighborhood* O *in* $\mathbb{R}^d$ *such that*

$$\lim_{h \to 0} \sum_{\Omega_e \in \mathcal{P}_h} \int_{\partial \Omega_e} \varphi \, \partial^\alpha u^h|_{\Omega_e} \mathbf{n} \, da = \mathbf{0} \tag{3.4}$$

for all test functions $\varphi \in C_0^\infty(O)$*, and* $|\alpha| \leq k - 1$*.*

Moreover, Stummel provides in [38] a number of counter-examples of elements which pass the patch tests of Irons and Strang, but which yield approximations which do not converge to the exact solution.

3.3.2.1 Weak Enforcement of Continuity

3.3.3 Stability

3.3.3.1 Restrictions on the Element Partition

3.3.4 Variational Consistency

3.3.4.1 Weak Enforcement of Consistency

Consider the variational formulation for the model solid mechanics problem:

Find $\mathbf{u} \in \mathcal{S} = \{\mathbf{u} \in H^1(\Omega), \mathbf{u} = \bar{\mathbf{u}} \ \forall \mathbf{x} \in \Gamma_u\}$ such that

$$\int_\Omega (T_{ij,j} + \rho b_i) v_i \, dv = 0 \tag{3.5}$$

for all $\mathbf{v} \in \mathcal{V} = \{\mathbf{v} \in H^1(\Omega), \mathbf{v} = \mathbf{0} \ \forall \mathbf{x} \in \Gamma_u\}$. Alternatively,

$$\int_\Omega T_{ij} v_{i,j} \, dv - \int_\Omega \rho b_i v_i \, dv = \int_{\Gamma_t} \bar{t}_i v_i \, da. \tag{3.6}$$

Now, let us contemplate a particular representation $v_i^h = \sum_{a=1}^N \varphi_a v_{ia}$, where $\mathbf{v}^h \in \mathcal{V}^h$ and $\mathcal{V}^h \subset \mathcal{V}$, resulting in

$$\int_\Omega T_{ij} \varphi_{a,j} \, dv - \int_\Omega \rho b_i \varphi_a \, dv = \int_{\Gamma_t} \bar{t}_i \varphi_a \, da \quad \forall i, a. \tag{3.7}$$

The above expression should be satisfied *exactly* when the exact solution $\mathbf{u}$ lies within the finite dimensional approximation space $\mathcal{S}^h \subset \mathcal{S}$. Given an exact solution $\bar{T}_{ij}$ arising from some prescribed $\bar{t}_i = \bar{T}_{ij} n_j$ and $\rho b_i = -\bar{T}_{ij,j}$, we may express

$$\int_\Omega \bar{T}_{ij} \varphi_{a,j} \, dv + \int_\Omega \bar{T}_{ij,j} \varphi_a \, dv = \int_{\partial \Omega} \bar{T}_{ij} n_j \varphi_a \, da \quad \forall i, a. \tag{3.8}$$

If $\bar{T}_{ij}$ can be written as a polynomial expansion, i.e.

$$\bar{T}_{ij}(\mathbf{x}) = \sum_{|\alpha|=0}^{k} \bar{T}_{ij\alpha}\mathbf{x}^{\alpha}, \tag{3.9}$$

then the α-th order variational consistency requirement asserts:

$$\int_{\Omega} \mathbf{x}^{\alpha}\varphi_{a,i}\, dv + \int_{\Omega} \mathbf{x}^{\alpha}_{,i}\varphi_a\, dv = \int_{\partial\Omega} \mathbf{x}^{\alpha} n_i \varphi_a\, da \quad \forall i, a. \tag{3.10}$$

This degree of consistency is required if the bi-linear form $B(u, v)$ on $\mathcal{S}$ and $\mathcal{V}$ is to determine uniqueness of any exact polynomial solutions contained within $\mathcal{S}$. Moreover, the above expression guarantees that any solution may be reasonably well approximated by low-order polynomials in the locality of the selected domain Ω.

Consequently, we may consider an application of the above consistency requirements to the entire problem domain Ω, or – more practically – we may enforce consistency up to the desired order on each element domain Ω_e. The element-local α-th order consistency equations follow:

$$\int_{\Omega_e} \mathbf{x}^{\alpha}\varphi_{a,i}\, dv + \int_{\Omega_e} \mathbf{x}^{\alpha}_{,i}\varphi_a\, dv = \int_{\partial\Omega_e} \mathbf{x}^{\alpha} n_i \varphi_a\, da \quad \forall i, a. \tag{3.11}$$

It should be emphasized that the consistency equations set forth are conditions which apply only to the test functions $\varphi_a \in \mathcal{V}^h$, and not to the trial functions $\phi_a \in \mathcal{S}^h$. The trial solution space must, however, be capable of reproducing all polynomial solutions (and their derivatives) up to some corresponding order k, such that $\mathbb{P}_k \subset \mathcal{S}^h$.

In most practical situations, it may not be possible to evaluate the integral expressions exactly. Instead, numerical quadrature rules must be defined, both on the element's interior, and on its boundary, such that

$$\int_{\Omega_e} f(\mathbf{x}) dv \approx \sum_{q=1}^{N_q} w_q f(\mathbf{x}_q), \tag{3.12}$$

$$\int_{\partial\Omega_e} f(\mathbf{x}) da \approx \sum_{b=1}^{N_b} w_b f(\mathbf{x}_b). \tag{3.13}$$

This yields yet another form of consistency, henceforth referred to as "quadrature consistency," expressed as:

$$\sum_{q=1}^{N_q} w_q \left[\mathbf{x}^{\alpha}_q \varphi^{(q)}_{a,i} + \mathbf{x}^{\alpha}_{q,i}\varphi^{(q)}_a\right] = \sum_{b=1}^{N_b} w_b \mathbf{x}^{\alpha}_b n^{(b)}_i \varphi^{(b)}_a \quad \forall i, a. \tag{3.14}$$

Moving forward in our developments, quadrature consistency will be the only form of consistency of practical interest, as it appropriately reflects the discrete data quantities at our disposal.

A brief remark should be made regarding the lack of equivalence between the exact evaluation of consistency in equation (3.11) and its numerical approximation in equation (3.14). In general, we cannot claim that satisfaction of one guarantees the other. There is only one occasion when we may say that (3.14) holds if and only if (3.11) is satisfied, which occurs only when sufficiently accurate quadrature rules are used on the element and its boundary. In the vast majority of situations, however, this is an impractical constraint, as the construction of high-order quadrature rules on arbitrary polyhedra (though possible) proves to be somewhat computationally intensive (see the literature by Sukumar, etc.). Moreover, without a precise representation of the test functions over the element domain, it becomes infeasible to consider an exact integration of such functions.

3.3.5 Numerical Quadrature Consistency

Beyond consistency with the weak form for a specified subspace of polynomial functions used to represent the solution, we also require that the numerical quadrature scheme utilized be sufficiently accurate to the extent that: Galerkin exactness is satisfied for certain classes of solutions, and that the quadrature error has a bound which is of a lower order than that of the approximation error.

3.3.5.1 Bubnov-Galerkin and Petrov-Galerkin Approaches

3.4 Specific Formulations

3.4.1 The Continuous-Galerkin PEM

3.4.2 The Weak-Galerkin PEM

3.4.3 The Discontinuous-Galerkin PEM

3.5 Enhancements to Improve Solution Accuracy

3.5.1 Partition-Based Enhancement Functions

3.5.2 Mixed PEM Discretizations

Chapter 4

An Implementational Framework for the PEM

Chapter 5

A Numerical Evaluation of the PEM

5.1 Convergence Analysis

5.2 Parameter Sensitivity Analysis

5.3 Computational Efficiency

5.3.1 Performance Comparison

5.4 Resistance to Locking Phenomena

Chapter 6

Conclusions and Future Work

Evaluate the efficacy of the proposed formulations within the presented context. Assess whether there really is a silver bullet to the locking problem, or if we can expect for locking to be an inherrent issue with any numerical approximation method.

Describe the nature of future work that will be done in this area of research.

References

[1] Ivo Babuška. Error-bounds for finite element method. *Numerische Mathematik*, 16:322–333, 1971.

[2] Ivo Babuška and Manil Suri. Locking effects in the finite element approximation of elasticity problems. *Numerische Mathematik*, 62:439–463, 1992.

[3] Ivo Babuška and Manil Suri. On locking and robustness in the finite element method. *SIAM Journal on Numerical Analysis*, 29(5):1261–1293, 1992.

[4] J. E. Bishop. A displacement-based finite element formulation for general polyhedra using harmonic shape functions. *International Journal for Numerical Methods in Engineering*, 97:1–31, 2014.

[5] Franco Brezzi. On the existence, uniqueness and approximation of saddle-point problems arising from lagrangian multipliers. *ESAIM: Mathematical Modelling and Numerical Analysis - Modlisation Mathmatique et Analyse Numrique*, 8:129–151, 1974.

[6] Jiun-Shyan Chen, Michael Hillman, and Marcus Rüter. An arbitrary order variationally consistent integration for galerkin meshfree methods. *International Journal for Numerical Methods in Engineering*, 95:387–418, 2013.

[7] H. Chi, L. Beirão da Veiga, and G. H. Paulino. Some basic formulations of the virtual element method (vem) for finite deformations. *Computer Methods in Applied Mechanics and Engineering*, 318:148–192, 2017.

[8] Heng Chi, Cameron Talischi, Oscar Lopez-Pamies, and Glaucio H. Paulino. A paradigm for higher-order polygonal elements in finite elasticity using a gradient correction scheme. *Computer Methods in Applied Mechanics and Engineering*, 306:216–251, 2016.

[9] L. Beirão da Veiga, F. Brezzi, A. Cangiani, G. Manzini, L. D. Marini, and A. Russo. Basic principles of virtual element methods. *Computer Methods in Applied Mechanics and Engineering*, 23:199–214, 2013.

[10] L. Beirão da Veiga, C. Lovadina, and D. Mora. A virtual element method for elastic and inelastic problems on polytope meshes. *Computer Methods in Applied Mechanics and Engineering*, 295:327–346, 2015.

[11] E. A. de Souza Neto, D. Perić, M. Dukto, and D. R. J. Owen. Design of simple low order finite elements for large strain analysis of nearly incompressible solids. *International Journal of Solids and Structures*, 33:3277–3296, 1996.

[12] C. R. Dohrmann and M. M. Rashid. Polynomial approximation of shape function gradients from element geometries. *International Journal for Numerical Methods in Engineering*, 53:945–958, 2002.

[13] Mohamed Salah Ebeida. Vorocrust v. 1.0, Jul 2017.

[14] Carlos A. Felippa. *Introduction to Finite Element Methods*. University of Colorado, Boulder, 2004.

[15] D. P. Flanagan and T. Belytschko. A uniform strain hexahedron and quadrilateral with orthogonal hourglass control. *International Journal for Numerical Methods in Engineering*, 17:679–706, 1981.

[16] Michael S. Floater. Mean value coordinates. *Computer Aided Geometric Design*, 20:19–27, 2003.

[17] Arun Gain, Cameron Talischi, and Glaucio H. Paulino. On the virtual element method for three-dimensional elasticity problems on arbitrary polyhedral meshes. *Computer Methods in Applied Mechanics and Engineering*, 282, 11 2013.

[18] Xifeng Gao, Wenzel Jakob, Marco Tarini, and Daniele Panozzo. Robust hex-dominant mesh generation using field-guided polyhedral agglomeration. *ACM Transactions on Graphics*, 36, 2017.

[19] Thomas J. R. Hughes. *The Finite Element Method–Linear Static and Dynamic Finite Element Analysis*. Dover Publications, 2000.

[20] Pushkar Joshi, Mark Meyer, Tony DeRose, Brian Green, and Tom Sanocki. Harmonic coordinates for character articulation. *ACM Transactions on Graphics*, 26, 2007.

[21] Nam-Sua Lee and Klaus-Jürgen Bathe. Effects of element distortions on the performance of isoparametric elements. *International Journal for Numerical Methods in Engineering*, 36:3553–3576, 1993.

[22] Qiaoluan H. Li and Junping Wang. Weak galerkin finite element methods for parabolic equations. *Numerical Methods for Partial Differential Equations*, 29:2004–2024, 2013.

[23] Guang Lin, Jiangguo Liu, and Farrah Sadre-Marandi. A comparative study on the weak galerkin, discontinuous galerkin, and mixed finite element methods. *Journal of Computational and Applied Mathematics*, 273:346–362, 2015.

[24] Richard H. MacNeal. A theorem regarding the locking of tapered four-noded membrane elements. *International Journal for Numerical Methods in Engineering*, 24:1793–1799, 1987.

[25] L. Mu, J. Wang, and Y. Wang. A computational study of the weak galerkin method for second-order elliptic equations. *Numerical Algorithms*, 63:753, 2013.

[26] L. Mu, J. Wang, and X. Ye. Weak galerkin finite element method for second-order elliptic problems on polytopal meshes. *International Journal of Numerical Analysis and Modeling*, 12:31–53, 2015.

[27] Lin Mu, Junping Wang, and Xiu Ye. A weak galerkin finite element method with polynomial reduction. *Journal of Computational and Applied Mathematics*, 285:45–58, 2015.

[28] Daniel Pantuso and Klaus-Jürgen Bathe. On the stability of mixed finite elements in large strain analysis of incompressible solids. *Finite Elements in Analysis and Design*, 28:83–104, 1997.

[29] M. M. Rashid and P. M. Gullett. On a finite element method with variable element topology. *Computer Methods in Applied Mechanics and Engineering*, 190:1509–1527, 2000.

[30] M. M. Rashid and A. Sadri. The partitioned element method in computational solid mechanics. *Computer Methods in Applied Mechanics and Engineering*, 237–240:152–165, 2012.

[31] M. M. Rashid and M. Selimotić. A three-dimensional finite element method with arbitrary polyhedral elements. *International Journal for Numerical Methods in Engineering*, 67:226–252, 2006.

[32] J.-F. Remacle, J. Lambrechts, B. Seny, E. Marchandise, A. Johnen, and C. Geuzainet. Blossom-quad: a non-uniform quadrilateral mesh generator using a minimum cost perfect matching algorithm. *International Journal for Numerical Methods in Engineering*, 89:1102–1119, 2012.

[33] Mili Selimotić. *Polyhedral Finite-Element Approximants in 3D Solid Mechanics*. PhD thesis, University of California, Davis, 2008.

[34] J. C. Simo and F. Armero. Geometrically non-linear enhanced strain mixed methods and the method of incompatible modes. *International Journal for Numerical Methods in Engineering*, 33:1413–1449, 1992.

[35] J. C. Simo, F. Armero, and R. L. Taylor. Improved versions of assumed enhanced strain tri-linear elements for 3d finite deformation problems. *Computer Methods in Applied Mechanics and Engineering*, 110:359–386, 1993.

[36] J. C. Simo and M. S. Rifai. A class of mixed assumed strain methods and the method of incompatible modes. *International Journal for Numerical Methods in Engineering*, 29:1595–1638, 1990.

[37] Friedrich Stummel. The generalized patch test. *SIAM Journal on Numerical Analysis*, 16(3):449–471, 1979.

[38] Friedrich Stummel. The limitations of the patch test. *International Journal for Numerical Methods in Engineering*, 16:177–188, 1980.

[39] N. Sukumar. Construction of polygonal interpolants: a maximum entropy approach. *International Journal for Numerical Methods in Engineering*, 61:2159–2181, 2004.

[40] Manil Suri. On the robustness of the h- and p-versions of the finite-element method. *Journal of Computational and Applied Mathematics*, 35:303–310, 1991.

[41] Theodore Sussman and Klaus-Jürgen Bathe. Spurious modes in geometrically nonlinear small displacement finite elements with incompatible modes. *Computers & Structures*, 140:14–22, 2014.

[42] Cameron Talischi and Glaucio H. Paulino. Addressing integration error for polygonal finite elements through polynomial projections: A patch test connection. *Mathematical Models and Methods in Applied Sciences*, 24:1701–1727, 2014.

[43] Cameron Talischi, Anderson Pereira, Ivan F. M. Menezes, and Glaucio H. Paulino. Gradient correction for polygonal and polyhedral finite elements. *International Journal for Numerical Methods in Engineering*, 102:728–747, 2015.

[44] Eugene L. Wachspress. *A Rational Finite Element Basis*. Academic Press, 1975.

[45] J. Wang and X. Ye. A weak galerkin finite element method for second-order elliptic problems. *Journal of Computational and Applied Mathematics*, 241:103–115, 2013.

[46] X. Wang, N.S. Malluwawadu, F. Gao, and T.C. McMillan. A modified weak galerkin finite element method. *Journal of Computational and Applied Mathematics*, 271:319–329, 2014.

[47] Robert Winkler. Comments on membrane locking. *Proceedings in Applied Mathematics and Mechanics*, 10:229–230, 2010.

Brian Doran Giffin
December 2017
Civil and Environmental Engineering

A Polytopal Element Framework for Improved Solution Accuracy and Robustness

Abstract

The abstract that is submitted to UMI must be formatted as shown in the example here. The body of the abstract cannot exceed 350 words. It should be in typewritten form, double-spaced, and on bond paper. It is important to write an abstract that gives a clear description of the content and major divisions of the dissertation, since UMI will publish the abstract exactly as submitted. Students completing their requirements under Plan A should provide extra copies of the typed summary for use by the dissertation committee during the examination.

The abstract that is submitted to UMI must be formatted as shown in the example here. The body of the abstract cannot exceed 350 words. It should be in typewritten form, double-spaced, and on bond paper. It is important to write an abstract that gives a clear description of the content and major divisions of the dissertation, since UMI will publish the abstract exactly as submitted. Students completing their requirements under Plan A should provide extra copies of the typed summary for use by the dissertation committee during the examination.

The abstract that is submitted to UMI must be formatted as shown in the example here. The body of the abstract cannot exceed 350 words. It should be in typewritten form, double-spaced, and on bond paper. It is important to write an abstract that gives a clear description of the content and major divisions of the dissertation, since UMI will publish the abstract exactly as submitted. Students completing their requirements under Plan A should provide extra copies of the typed summary for use by the dissertation committee during the examination.

The abstract that is submitted to UMI must be formatted as shown in the example here. The body of the abstract cannot exceed 350 words. It should be in typewritten form,

form, double-spaced, and on bond paper. It is important to write an abstract that gives a clear description of the content and major divisions of the dissertation, since UMI will publish the abstract exactly as submitted. Students completing their requirements under Plan A should provide extra copies of the typed summary for use by the dissertation committee during the examination.